New Emerging Inorganic-Organic Systems for Drug-Delivery: Hydroxyapatite@Furosemide Hybrids

Marzia La Rocca
Alessia Rinaldi
Giovanna Bruni
Valeria Friuli
Lauretta Maggi
Marcella Bini (bini@unipv.it)
Universita degli Studi di Pavia https://orcid.org/0000-0001-7099-0650

Research Article

Keywords: Hydroxyapatite, Furosemide, Drug-delivery, XRPD, FT-IR, Dissolution Tests, Wettability

Posted Date: February 1st, 2022

DOI: https://doi.org/10.21203/rs.3.rs-1305809/v1

Version of Record: A version of this preprint was published at Journal of Inorganic and Organometallic Polymers and Materials on March 20th, 2022. See the published version at https://doi.org/10.1007/s10904-022-02302-3.

Abstract

In the pharmaceutical market, the need to find effective systems for the efficient release of poorly bioavailable drugs is a forefront topic. The inorganic–organic hybrid materials have been recognized as one of the most promising systems. In this paper, we developed new Hydroxypapatite@Furosemide hybrids with improved dissolution rates in different media with respect to the drug alone. The hybrids formation was demonstrated by SEM/EDS measurements (showing homogeneous distribution of the elements) and FT-IR spectroscopy. The drug was adsorbed onto hydroxyapatite surfaces in amorphous form, as demonstrated by XRPD and its thermal stability was improved due to the absence, in the hybrids, of melting and decomposition peaks typical of the drug. The Sr substitution on Ca sites in hydroxyapatite allows increasing the surface area and pore volume, foreseeing a high capacity of drug loading. The dissolution tests of the hybrid compounds show dissolution rates much faster than the drug alone in different fluids, and also their solubility and wetting ability is improved in comparison to furosemide alone.

1. Introduction

The search for effective systems increasing the bioavailability of drugs by improving the physico-chemical and/or biopharmaceutical properties is a fascinating and forefront topic, particularly appealing for poorly soluble drugs administered in oral form, the most common way for chronic therapies requiring repeated administrations. The design of materials constituted by host inorganic matrices and drug guests has attracted considerable attention and is one of the latest research strategies in the development of new drug alternatives in the pharmaceutical industry [1–5].

Furosemide (*Fur*), 4-chloro-2-[(2-furanylmethyl)-amino]-5-sulfamoylbenzoic acid, is a high ceiling loop diuretic drug to treat edema and hypertension linked to congestive heart failure, cirrhosis of the liver and renal disease. According to the Biopharmaceutics Classification System (BCS), furosemide belongs to class IV drug, characterized by low solubility and permeability values [6]. Indeed, furosemide is almost insoluble in water (6 mg L^{-1}), resulting in significant intra-individual variations in absorption and very poor oral bioavailability. It has a weak acidic nature, a short half-life (1-3 h) and poor bioavailability (60-65%) since this molecule is preferentially absorbed in the gastric mucosa and upper intestine, where the drug shows the lowest solubility (5-20 μg/ml). *Fur* exists in different polymorphic forms, showing variable dissolution rates [7, 8].

Despite some drawbacks, *Fur* shows great efficacy, and is highly used in therapeutics worldwide. However, high doses or prolonged use can lead to fluid and electrolyte imbalance which can provoke headaches, cramping, thirst, and weakness [9]. So, for the pharmaceutical industry, the developing of new oral formulations is mandatory for the improvement of its release to minimise the dose size so reducing side effects.

Numerous successful attempts were reported in the literature. Mesoporous materials [10, 11], surfactant-based methods [12], Na and K salts [13], cocrystals of *Fur* with a variety of co-formers, as well as hydrates and solvates [14–17] have been reported. Among the cited approaches to improve the dissolution rate of furosemide, the use of inorganic–organic hybrid materials has been recognized as one of the most promising systems.

Hydroxyapatite (*HAP*), $Ca_{10}(PO_4)_6(OH)_2$, is the main constituent of biological tissues such as bones and teeth. It has several intriguing features, such as good biocompatibility, biodegradability, osteogenisis, osteoconductivity and bioactivity, and can form direct bonds with living tissues [18]. In form of nanocrystals, *HAP* has unique properties, *i.e.* high surface to volume ratio, reactivity and biomimetic morphologies compared to the bulk counterpart due to quantum size effects and surface phenomena at the nanoscale. *HAP* nanocrystals can be used for example in tissue engineering, nanomedicine, industrial catalysis and in orthopaedic implant coating [19, 20]. In addition, *HAP* nanospheres thanks to their low solubility in physiological conditions can be used as carriers for controlled and local drug delivery both by surgical placement and injection [21, 22]. The drug delivery from hydroxyapatite minimizes the toxicity to other organs reducing the drug concentration in the blood, avoiding repeated dosage of drugs. *HAP* easily binds to both positive and negative molecules by simple adsorption and is used for delivery of molecules like antibiotics, contraceptives, acetylsalicylic acid, hormones, insulin and anticancer drugs [23–25]. The *HAP* doping/substitution with different kind of elements (Mg, Si, Sr, Eu, Zn, Ce..) was proposed as a way to improve the drug loading [26–28].

In this work, we propose, for the first time, a drug-delivery system based on the adsorption of Furosemide onto *Pure* and *Sr*-substituted Hydroxyapatite. The hybrids characterization was performed by the combined use of X-ray powder diffraction (XRPD), differential scanning calorimetry (DSC), and infrared spectroscopy (FT-IR), particularly useful to prove the presence of the drug onto *HAP* surface/pores. Scanning electron microscopy (SEM) coupled with energy dispersive X-ray spectroscopy (EDS) microanalysis supported the formation of the hybrids. The measure of contact angle of the powders, the solubility and the in vitro dissolution tests, performed in different media simulating the gastro-intestinal environment, demonstrated the effectiveness of the hybrids for the improvement of drug wettability and dissolution rate.

2. Materials And Methods

2.1. Syntheses

2.1.1. Synthesis of hydroxyapatite

Hydroxyapatite was synthesized by means of co-precipitation method. $Ca(NO_3)_2$ 4 H_2O and $(NH_4)_2HPO_4$ in the proper stoichiometric amount were dissolved in two different beckers in distilled water (15 ml) and basified with NH_4OH until pH~10 was reached. After 15 min of stirring, the solution of phosphate was poured drop by drop in that of calcium, then the pH was checked and, if necessary, adjusted to 10 with

ammonium hydroxide. After 30 min of stirring, the temperature was raised to 80°C and maintained for 1h. After cooling to room temperature, the solution was centrifuged, and the collected powder was washed three times with deionized water, then transferred in oven at 100°C for 22 h. This sample will be named *HAP-Pure*.

2.1.2. Synthesis of Sr-doped $Ca_6Sr_4(PO_4)_6(OH)_2$ hydroxyapatite

$Ca(NO_3)_2\ 4H_2O$, $Sr(NO_3)_2$ and $(NH_4)_2HPO_4$ in the proper stoichiometric amounts to obtain $Ca_6Sr_4(PO_4)_6(OH)_2$, were dissolved in three different beckers in distilled water (10 ml each one) and basified with NH_4OH until pH~10 was reached. After 15 min of stirring, the solution of Sr was poured drop by drop in that of calcium and the pH was checked and eventually adjusted to 10 with ammonium hydroxide. Then, the solution of phosphate was poured into that of calcium/strontium with the control of pH. After 30 min of stirring, the temperature was raised to 80°C and maintained for 1h. At the end, after cooling to room temperature, the solution was centrifuged, and the powder washed with deionized water and treated in oven at 100°C for 22 h. This sample will be named *HAP-Sr*.

2.1.3. Synthesis of HAP@Furosemide hybrids

Furosemide (*Fur*), Formula $C_{12}H_{11}ClN_2O_5S$ (Scheme I), was gently donated by Fabbrica Italiana Sintetici S.p.A., Vicenza, Italy.

Furosemide was dissolved into a mixture of ethanol:water (3:1 ratio) (drug concentration 10 mg/ml, 10 ml overall). Then, 150 mg of *HAP-Pure* or *HAP-Sr* was added to the drug solution and maintained for 24 h at ambient temperature under continuous stirring. Then, the powder was centrifuged, dried at room temperature, and maintained in desiccator for the subsequent use. In the following, the samples will be named *HAP-Pure-Fur* and *HAP-Sr-Fur.*

2.2. Techniques

2.2.1. Physico-chemical measurements

XRPD measurements were performed by using a Bruker D5005 diffractometer (Bruker BioSpin, Fällanden, Switzerland) with the Cu Kα radiation, graphite monochromator and scintillation detector. The patterns were collected in air with a step size of 0.03° and counting time of 2s per step in the angular range 5-70° (*Hybrids*), 5-35° (*Fur*) and 10-70° (*HAPs*) by using a low background silicon sample holder.

FT-IR spectra were obtained with a Nicolet FT-IR iS20 spectrometer (Nicolet, Madison, WI, USA) equipped with ATR (Attenuated Total Reflectance) sampling accessory (Smart iTR with diamond plate) by co-adding 32 scans in the 4000–650 cm^{-1} range at 4 cm^{-1} resolution.

DSC measurements were carried out by a DSC Q2000 apparatus interfaced with a TA 5000 data station (TA Instruments, New Castle, DE, USA). The instrument was calibrated using ultrapure (99.999%) indium

(m.p. = 156.6°C; ΔH =28.54 J g^{-1}) as standard. The calorimetric measurements were conducted up to 250°C at a heating rate of 5 K min^{-1} on samples amount of about 3-5 mg in open standard aluminium pans under nitrogen flow (45 mL·min^{-1}).

SEM images were collected by a Zeiss Evo MA10 (Carl Zeiss, Oberkochen, Germany) microscope coupled with the EDS detector for microanalysis (X-max 50 mm, Oxford Instruments). The samples for SEM analysis were sputtered with a thin layer of gold and analysed at an acceleration voltage of the electron beam of 20 kV. The EDS data were obtained on pristine samples (not sputtered).

N2 adsorption isotherms were collected on samples, previously evacuated overnight at room temperature. Use was made of a Porosimeter (Thermoelectron Model Sorptomatic 1990, Waltham, Massachusets, United States). The data were analysed with the Brunauer, Emmett, and Teller (BET) algorithm to determine the surface area and pores' volume.

2.2.2. Pharmaceutical measurements

The Furosemide content in the *HAP-Pure-Fur and HAP-Sr-Fur* samples was determined in the conditions in which the drug is highly soluble, *i.e* phosphate buffer pH=5.8. In the same conditions, a calibration curve was previously performed at 274 nm, 1 cm cell, obtaining a correlation coefficient of 0.9999. At this wavelength, the carrier Hydroxyapatite does not show any absorption.

It was not possible to determine the thermodinamic solubility of the hybrid compounds with the shake flask method, because the carrier is insoluble in water and thus it was not feasible to establish when a saturated solution of *Fur* is reached. So, we wheighed samples corresponding to at least four times the drug dose (100 mg/L) in the flasks, that were maintained under magnetic stirring at 300 rpm, at 21°C. Then we measured the *Fur* absorbance, after different time intervals, on filtered portion (0.45 µm) of the supernatant solution, to verify if all the quantity of considered drug was completely dissolved.

The wettability of the samples was determined by measuring the contact angle θ (deg). Contact Angle Meter DMe-211Plus (NTG Nuova Tecnogalenica, Cernusco, Italy) was used for contact angle determination: a 9µl drop of fluid (deionized water, pH 1.0 hydrochloric acid solution or pH 5.8 buffer) was extruded from the needle and dropped onto the solid surface of the powder. Photos were recorded at progressive times and the contact angle was measured by the software provided. Three replicas for each sample were performed. These measurements provide evidence of the attitude of the solid samples to be wetted by the considered fluids.

For the dissolution test, all the samples were sieved through a 400-mesh grid and then samples corresponding to 25 mg of *Fur* were weighed. The dissolution test was performed using paddle method (Erweka DT-D6, Dusseldorf, Germany) at 37.0 ± 0.5°C, 50 rpm, in 900 mL of pH 5.8 buffer, medium required by the US Pharmacopeia [29], and in other two fluids: hydrochloric acid solution, pH 1.0, to simulate fasting gastric conditions and deionized water (pH 6.8), to simulate neutral condition (n=3

repetitions). The dissolution media were prepared following the reagents and buffer solutions section of the USP [30].

The amount of drug dissolved was determined by UV detection, on filtered portions of the dissolution fluid, at 274 nm with a spectrophotometer (Lambda 25; Perkin-Elmer) and the data were processed by a suitable software (Winlab V6 software, Perkin-Elmer, Monza, Italy).

3. Results And Discussion

3.1. Physico-chemical characterization

The X-ray powder diffraction patterns of pure Furosemide drug and *HAPs*, as well as those of *HAPs@Fur* hybrids are shown in Figure 1. Furosemide is a crystalline material (Figure 1A), whose pattern well agrees with that reported in the literature and attributed to Form I [7, 31, 32]. The *HAP-Pure* sample reflections (Figure 1B) are in very good agreement with the peak positions expected for $Ca_{10}(PO_4)_6(OH)_2$ compound (Card N. 74-0565), with a hexagonal lattice and the $P6_3/m$ space group. The same is true for *HAP-Sr* sample: its pattern is well comparable with that of *HAP-Pure*, apart a shift to lower angles of all the peak positions. This is due to the difference of the ionic radii of Sr and Ca ions (1.18 and 1.31 Å with respect to 1 and 1.18 Å for the six and nine coordination environments respectively for the two cationic sites in *HAP*), justifying the lattice expansion [33]. In addition, the pattern of *HAP-Sr*, with broader and less defined peaks with respect to *HAP-Pure*, is suggestive of a low crystallinity, notwithstanding the same synthesis conditions. An effect of the Sr ions on the kinetic of the synthesis can be supposed. The XRPD patterns of the hybrids are practically over imposable to the corresponding patterns of *HAPs*: all the peaks pertain to the *HAP* phase alone, no peaks due to Furosemide can be evidenced. This can be due to the presence of Furosemide in amorphous form. However, from these evidences, it is clear that the only XRPD data are not able to confirm the hybrids formation, but other kind of analysis, particularly spectroscopic or compositional ones, are required to prove the Furosemide presence on *HAP* surfaces. However, an indirect proof of the presence of Furosemide on the *HAP* particles could be represented by the reduction of the intensities of the reflections of the entire hybrids' patterns with respect to the corresponding *HAPs*: this evidence could be related to the coverage of *HAP* particles with a sort of a coating layer of drug.

The spectroscopic analysis could provide useful insights into the Furosemide adsorption onto the *HAP* nanoparticles. The FT-IR spectra of *Fur, HAP-Pure, HAP-Sr* and the hybrids *HAP-Pure-Fur* and *HAP-Sr-Fur* are reported in the ranges 4000-2000 cm^{-1} and 2000-650 cm^{-1} in Figures 2A and 2B, respectively.

The spectrum of the pure Furosemide drug well agrees with the literature data of the polymorphic Form I, in agreement also with XRPD findings [32]. *Fur* exhibits the main vibrational frequencies at 3396 and 3278 cm^{-1} (sulphonamide primary amine stretching), 3348 cm^{-1} (secondary amine stretching), 1667 cm^{-1} (carboxyl stretching), 1590 and 1559 cm^{-1} (N-H bending vibrations), and 1315 and 1139 cm^{-1} (SO_2 asymmetric and symmetric stretching).

The *HAP-Pure* FT-IR spectrum too well agrees with those reported in the literature for Hydroxyapatite [34]. In this case, few bands are observed in the analysed FT-IR range: the sharp band at 3568 cm^{-1} is assigned to the OH stretching mode, the bands at 1088 and 1022 cm^{-1} are due to P-O antisymmetric stretching modes and that at 962 cm^{-1} to P-O symmetric stretching mode. The *HAP-Sr* spectrum is like that of *HAP-Pure*: the bands due to P-O bonds slightly shift to lower wavenumbers, due to the higher reduced mass of the harmonic oscillator related to the Sr presence. In addition, the band at 3568 cm^{-1} is very low, substituted by a broader band however attributable to OH vibration. This can be due to the increase of lattice parameters because of Sr substitution and the formation of an open structure about the OH groups, reducing the crystal force field and increasing the mixing of the OH vibrational and translational motions.

In the FT-IR spectra of the hybrids (Figure 2A and B), together with the bands previously commented of *HAP-Pure* and *HAP-Sr* samples, some small peaks attributable to the drug are visible particularly in the range 1600-1200 cm^{-1}. The band at about 1610 cm^{-1}, well evident in both the samples, is compatible with the hydrogen bonds formation between *HAP* and *Fur*. Other low bands typical of the drug are also shifted with respect to those of the *Fur* alone, suggesting a complex hydrogen bonding scheme in the hybrid compounds.

Thermal data, in particular the melting or decomposition temperatures of drugs, can be employed to prove the formation of new compounds, because of drug adsorption [3–5]. The DSC curves of *Fur*, *HAP-Pure-Fur*, and *HAP-Sr-Fur* are reported in Figure 3. The curve of *Fur* agrees with the literature, the following thermal effects are present: a small endothermic peak at about 135°C, due to the solid-solid phase transition between Form I, the low temperature stable form, and a high temperature stable form [31], in enantiotropic relationship; a complex endothermic-exothermic thermal signal which indicates a melting-decomposition process of the drug at about 217°C.

HAP, as other anologous inorganic compounds, has a high structural stability in this temperature range and, as expected, no thermal events are present [35].

The DSC traces of both hybrids are similar (Figure 3): a flat curve, without any thermal event, apart a broad band at low temperature due to water desorption, is observed, proving that the Furosemide turned out to be amorphous and stable to decomposition, because of its adsorption onto the *HAP* surfaces.

The morphological characterization was performed by SEM microscopy. The micrographs of *Fur*, *HAP-Pure* and *HAP-Sr* and those of the hybrids are shown in Figures 4A-E. *Fur* is made of flattened sticks with length ranging from one micron to a few tens of micron (Fig. 4A). *HAP-Pure* occurs in the form of dense aggregates of small, rounded particles (Fig. 4B) and the same is true for *HAP-Sr* (Fig. 4C), whose particles seem smaller and less compact with respect to the pure *HAP*. The adsorption measurements, in the BET portion, allowed determining a surface area and pore volume of 357 m^2/g and 0.24 cm^3/g for *HAP-Sr* with respect to 143 m^2/g and 0.08 cm^3/g for *HAP-Pure*. The areas are very high, if compared to analogous samples prepared by similar synthesis routes [23, 24], suggesting the formation of highly

microporous hydroxyapatites. An effect of Sr substitution is obviously evident on both surface area and pore volume, due to the same kind of synthesis. These features could be positive for the subsequent drug loading, which could be, in principle, expected to be higher for *HAP-Sr* sample.

The hybrids' morphologies resemble those of the corresponding *HAP* samples (Fig. 4D, E): aggregates of small, rounded particles are again well evident, confirming that the adsorption of furosemide does not change the external morphology. No particles attributable to pure drug are visible.

The EDS microanalysis, combined with SEM, is a widespread tool to check the homogeneity of cations distribution, and therefore, in our case, to support the hybrids formation by analysing the presence of the characteristic elements of *HAP* (Ca and P ions, and Sr substituent) and Furosemide (Cl and/or S ions). The elemental maps obtained for the hybrid compounds show a good homogeneous distribution of all the elements and show that Cl and S (not shown) ions are located in the same points of the powders, where also Ca and P are mainly concentrated (Figure 5). This observation obviously supports the hybrids' formation. For all the samples, the EDS spectra allowed to determine the chemical compositions, which were found in very good agreement with the expected stoichiometries: Ca/P ratio is near to the ideal value 1.67, and the Sr substituent is present in the expected amount (Table 1). The peaks of S and Cl, both elements present in the Furosemide molecule, confirm the existence of the drug in the analysed samples. Their amount, in both the hybrids, is the same, due to the presence of 1 Cl and 1 S atoms in the furosemide molecule. From the atomic ratios (Table 1) we can calculate a drug loading of about 9.1 wt% and 8.3 wt% for *HAP-Sr-Fur* and *HAP-Pure-Fur* respectively. These data will be compared with the amount of drug loading determined by UV-Vis spectroscopy (see par. 3.2).

Table 1
– Atomic percentages of the elements obtained by EDS analysis

	Ca	P	Sr	S	Cl
HAP-Pure	17.89	11.55	-	-	-
HAP-Sr	8.99	8.04	6.01	-	-
HAP-Pure-Fur	10.17	6.70	-	0.27	0.28
HAP-Sr-Fur	4.82	5.05	3.41	0.26	0.29

3.2. Pharmaceutical characterization

The drug loading was determined to be 8.2 ± 1.0% for *HAP-Sr-Fur* and 7.2 ± 0.8% for *HAP-Pure-Fur* and these values are in good agreement with those obtained from the EDS microanalyses (Table 1).

From the solubility experiment, it was possible to determine that, for both hybrids, the *Fur* solubility is greater than four times the dose (corresponding to 100 mg L^{-1}), and much higher than the solubility of

Fur alone (6 mg L^{-1}) [6].

The contact angles measured for *HAP-Pure-Fur* and *HAP-Sr-Fur* in the different fluids show an increased wetting ability compared to *Fur* alone. This effect is immediately evident at 1 sec after deposition (Figure 6), but increases more significantly over time (Figure 7) in all the media considered. *HAP-Sr-Fur* starts from values of 45-55° θ, which are lower compared to *HAP-Pure-Fur*, 55-65° θ, and both are at least half the values obtained from *Fur* alone. Moreover, the contact angles of the two hybrids decrease quickly with time to 10-20° θ in few seconds, showing a fast wetting ability, also explaining their more rapid dissolution behaviour (see Figure 8). On the other side, the contact angle of the drug remains constant throughout all the experiment (300 sec) (Figure 7).

The dissolution tests (Figure 8) confirm the improved performances of the two hybrid compounds in comparison with the drug alone in all the fluids considered. *Fur* is quite insoluble at pH=1 (simulating fasted gastric environment), but even in this condition *HAP-Pure-Fur* and *HAP-Sr-Fur* showed a very fast dissolution rate of the drug reaching 90% of the dose dissolved in about 120 min. Even more evident is the improvement of the drug dissolution rate from the two hybrids in the fluid prescribed by the US Pharmacopoeia, pH=5.8 buffer, in which the dose is delivered completely in less than 20 min. Only in the unbuffered condition (deionised water) a slight difference in the dissolution profile between *HAP-Pure-Fur* and *HAP-Sr-Fur* can be noticed, probably due to the faster wettability of this last compound. In any cases, both hybrids are able to greatly improve the *Fur* dissolution rate even in the neutral condition compared to the drug alone.

Our results represent a great improvement on the state of the art of furosemide drug delivery systems. In fact, our dissolution profiles in acidic medium (pH=1) are similar or even better than those reported for inorganic-organic hybrids based on silica particles [10–12], which however do not report tests in the conditions suggested by Pharmacopoeia (pH=5.8).

Furosemide, as already discussed, is characterized by a considerable variability in the intensity of the effect, due to its low solubility linked to the medium pH and to a very variable oral bioavailability. For this reason, the enhanced dissolution rate of *Fur* in the different fluids is a great advantage especially in the therapy of critical diseases when the effect should be reached as soon as possible.

4. Conclusions

The successful loading of Furosemide onto *HAP* surfaces was proved with the combined use of different experimental techniques. The Sr doping greatly increased the surface area of the *HAP*, but only slightly increased the drug loading with respect to pure HAP. This can be due to the formation of micro-porosity that does not fit well with Furosemide sizes. However, the new hybrids show greatly improved pharmaceutical properties with respect to Furosemide alone in terms of solubility, wettability and dissolution rate in all the fluids considered to simulate the gastro-intestinal environment. These characteristics could enhance the bioavailability of the drug and promote a quick appearance of the

therapeutic effect. This is particularly useful in critical pathologies when it is necessary to rapidly decrease the blood pressure of the patient. Notwithstanding the obtained drug loading is fairly low, the adsorption of drugs onto *HAP* surface was however revealed a winning strategy. Through the optimization of *HAP* surfaces and porosity, highly performing systems based on *HAP* hosts could be developed in future for different poorly soluble drugs.

Declarations

Acknowledgement

The authors are grateful to Prof. Vittorio Berbenni for the surface area measurements.

Funding

This research did not receive any specific grant from funding agencies in the public, commercial, or not-for-profit sectors.

CRediT author statement

Marzia La Rocca and Alessia Rinaldi: Investigation, Methodology; Giovanna Bruni, Valeria Friuli, Lauretta Maggi: Investigation, Validation, Formal analysis, Writing-Review & Editing; Marcella Bini: Conceptualization, Supervision, Writing - Original Draft.

Data availability

The datasets generated during the current study are available from the corresponding author on reasonable request.

References

1. S. Inocencio, T. Cordeiro, I. Matos, F. Danede, J.C. Sotomayor, I.M. Fonseca, N.T. Correia, M.C. Corvo, M. Dionísio, Microporous Mesoporous Mater. **310**, 110541 (2021)
2. E. Sayed, C. Karavasili, K. Ruparelia, R. Haj-Ahmad, G. Charalambopoulou, T. Steriotis, D. Giasafaki, P. Cox, N. Singh, L.-P.N. Giassafaki, A. Mpenekou, C.K. Markopoulou, I.S. Vizirianakis, M.-W. Chang, D.G. Fatouros, Z. Ahmada, J. Controlled Release **278**, 142 (2018)
3. M. Bini, F. Monteforte, I. Quinzeni, V. Friuli, L. Maggi, G. Bruni, J. Solid State Chem. **272**, 131 (2019)
4. D. Capsoni, I. Quinzeni, G. Bruni, V. Friuli, L. Maggi, M. Bini, J. Pharm. Sci. **107**, 267 (2018)
5. M. Guagliano, F. Monteforte, G. Bruni, V. Friuli, L. Maggi, I. Quinzeni, M. Bini, Appl. Clay Sci. **198**, 105826 (2020)
6. C.T. –, Supuran, Current Pharm. Design **14**, 641 (2008)
7. N.J. -, S. Babu, R. Cherukuvada, A. Thakuria, Nangia, Cryst. Growth Des. **10**, 1979 (2010)

8. M.M. -, J.G. Devilliers, A.P. Van Der Watt, W. Lotter, T.G. Liebenberg, Dekker, Drug Dev. Ind. Pharm. **21**, 1975 (1995)
9. F. Carta, C.T. Supuran, Expert opinion on therapeutic patients **23**, 681 (2013)
10. V. Ambrogi, L. Perioli, C. Pagano, F. Marmottini, M. Ricci, A. Sagnella, C. Rossi, European J. Pharm. Sci. **46**, 43 (2012)
11. V. Ambrogi, L. Perioli, C. Pagano, L. Latterini, F. Marmottini, M. Ricci, C. Rossi, Microporous Mesoporous Mater. **147**, 343 (2012)
12. A. Zvonar, K. Berginc, A. Kristl, M. Gasperlin, Int. J. Pharm. **388**, 151 (2010)
13. U.B. -, S. Rao Khandavilli, N. Gangavaram, S. Rajesh Goud, S. Cherukuvada, A. Raghavender, S.G. Nangia, S. Manjunatha, S. Nambiar, Pal, Cryst. Eng. Comm. **16**, 4842 (2014)
14. N.R. -, S. Goud, K. Gangavaram, S. Suresh, S.G. Pal, S. Manjunatha, A. Nambiar, Nangia, J. Pharm. Sci. **101**, 664 (2012)
15. B.I. Harriss, L. Vella-Zarb, C. Wilson, I. Radosavljevic, Evans, Cryst. Growth Des. **14**, 783 (2014)
16. V.K. Srirambhatla, A. Kraft, S. Watt, A.V. Powell, Cryst. Eng. Comm. **16**, 9979 (2014)
17. T. -, N. Ueto, N. Takata, A. Muroyama, A. Nedu, S. Sasaki, K. Tanida, Terada, Cryst. Growth Des. **12**, 485 (2012)
18. V. Bystrov, E. Paramonova, L. Avakyan, J. Coutinho, N. Bulina, Nanomaterials **11**, 2752 (2021)
19. A. García, M.V. Cabañas, J. Peña, S. Sánchez-Salcedo, Pharmaceutics **13**, 1981 (2021)
20. R. Rial, M. González-Durruthy, Z. Liu, J.M. Ruso, Molecules **26**, 3190 (2021)
21. S. Mofakhami, E. Salahinejad, J. Controlled Release **338**, 527 (2021)
22. S.L. –, W. Ochoa, C.E. Ortega-Lara, Guerrero-Beltrán, Pharmaceutics **13**, 1642 (2021)
23. X. Ding, J. Zheng, F. Ju, L. Wang, J. Kong, J. Feng, T. Liu, Ceram. Int. **47**, 34836 (2021)
24. R.C.R. –, G.F. dos Apostolos, W.M. Andrade, D. da Silva, M.C. de Assis Gomes, E.M.B. de Miranda, de Sousa, Int. J. Appl. Ceram. Technol. **16**, 1836 (2019)
25. S. -, S. Saber-Samandari, M. Saber-Samandari, F.C. Gazi, E. Cebeci, Talasaz, J Macromol. Sci. Part A **50**, 1133 (2013)
26. A. Alves Barbosa, S. Alves Júnior, R.L. Mendes, R. Santana, A. de Lima, de Vasconcelos, Ferraz, Mat. Sci. & Eng. C **116**, 111227 (2020)
27. Y. –, L. Xu, L. An, L. Chen, D. Cao, G. Zeng, Wang, Mat. Chem. Phys. **214**, 359 (2018)
28. M. –, A. Vila, A. García, M. Girotti, J.C. Alonso, A. Rodríguez-Cabello, J.A. González-Vázquez, E. Planell, J. Engel, N. Buján, M. García-Honduvilla, Vallet-Regí. Acta Biomater. **45**, 349 (2016)
29. Furosemide tablets/official monographs. In: The United States Pharmacopeia (USP41-NF36). Rockville, MD: United States Pharmacopeial Convention, Inc; 2018 pp.1894–95
30. Reagents. Solutions/Buffer solutions. The United States Pharmacopeia (USP40 -NF35). United States Pharmacopeial Convention, Inc., Rockville, MD; 2017. pp. 2409-2411
31. Y. -, E. Matsuda, Tatsumi, Int. J. Pharm. **60**, 11 (1990)

32. C. -, P. Doherty, York, Int. J. of Pharmaceutics **47**, 141 (1988)
33. R.D. -, Shannon, Acta Crystallogr. **A32**, 751 (1976)
34. B.O. -, Fowler, Inorg. Chem. **13**, 194 (1974)
35. H. Wang, L. Zhai, Y. Li, T. Shi, Mat. Res. Bull. **43**, 1607 (2008)

Schemes

Scheme 1 is available in the Supplementary Files section.

Figures

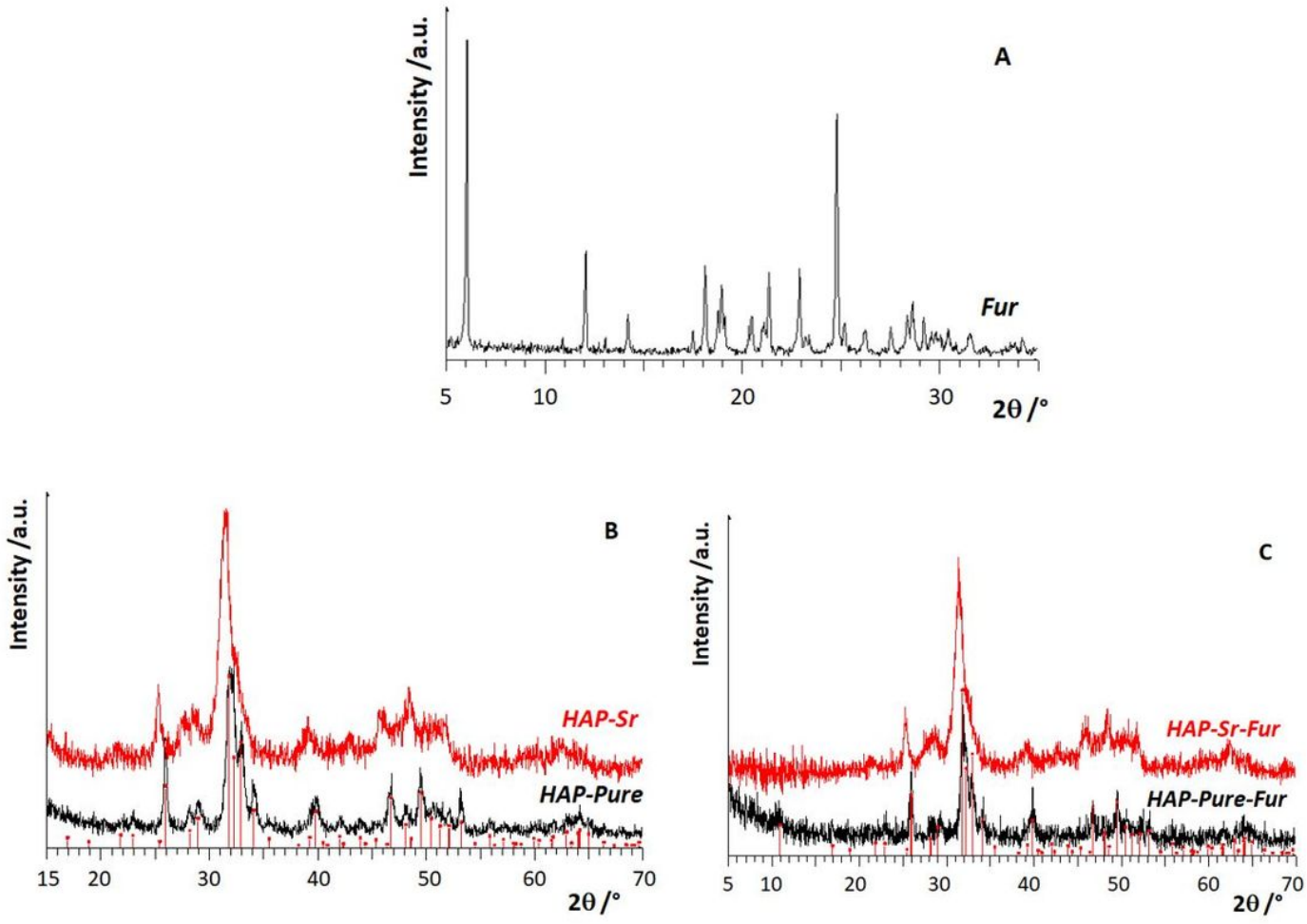

Figure 1

XRPD patterns of (A) *Fur*, (B) *HAPs* and (C) *HAPs@Fur* hybrids. The red bars in (B) and (C) refer to the expected peak positions of Hydroxyapatite (Card N. 74-0565).

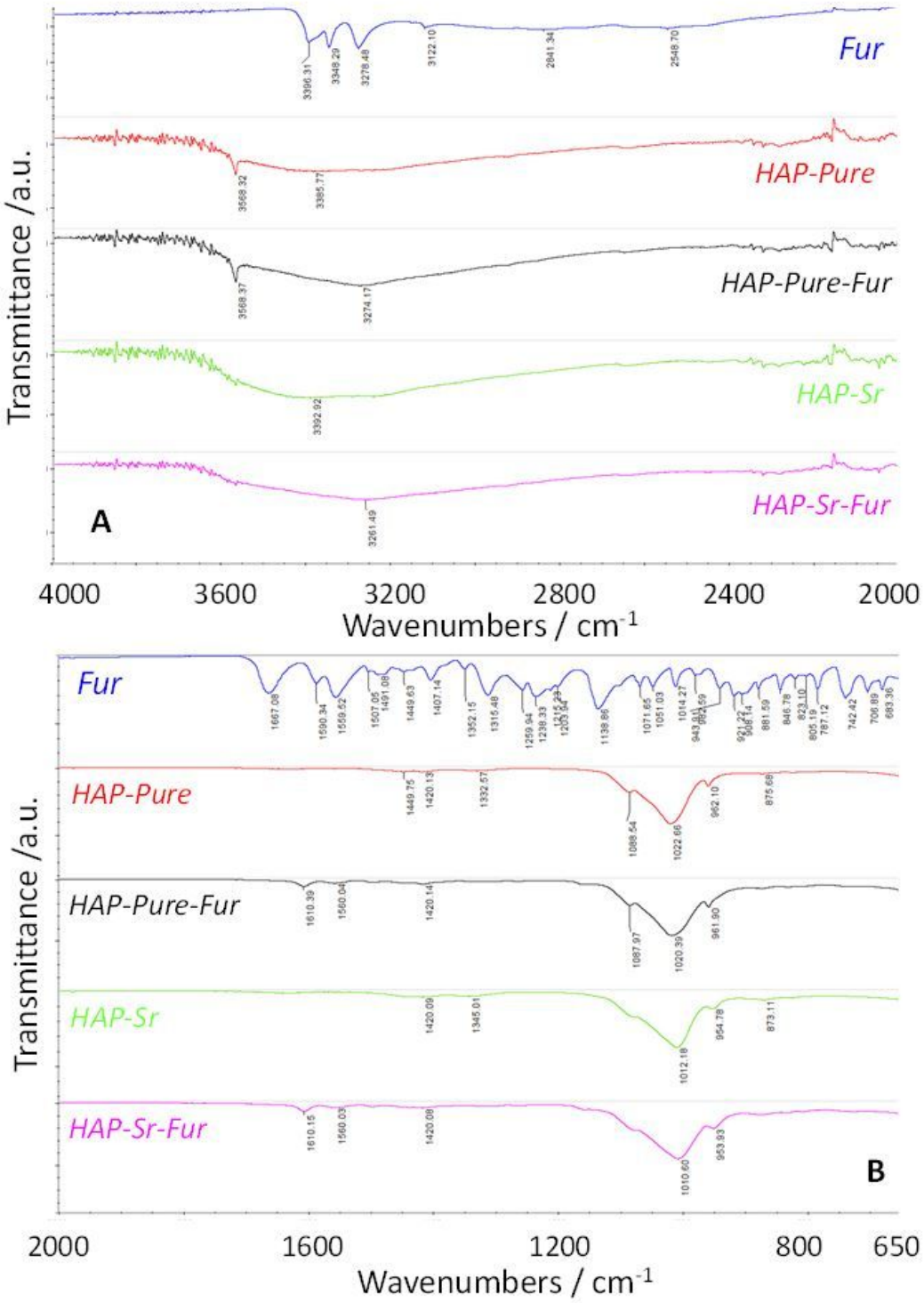

Figure 2

FT-IR spectra of the indicated samples in the 4000-2000 cm^{-1} (A) and 2000-650 cm^{-1} (B) spectral ranges.

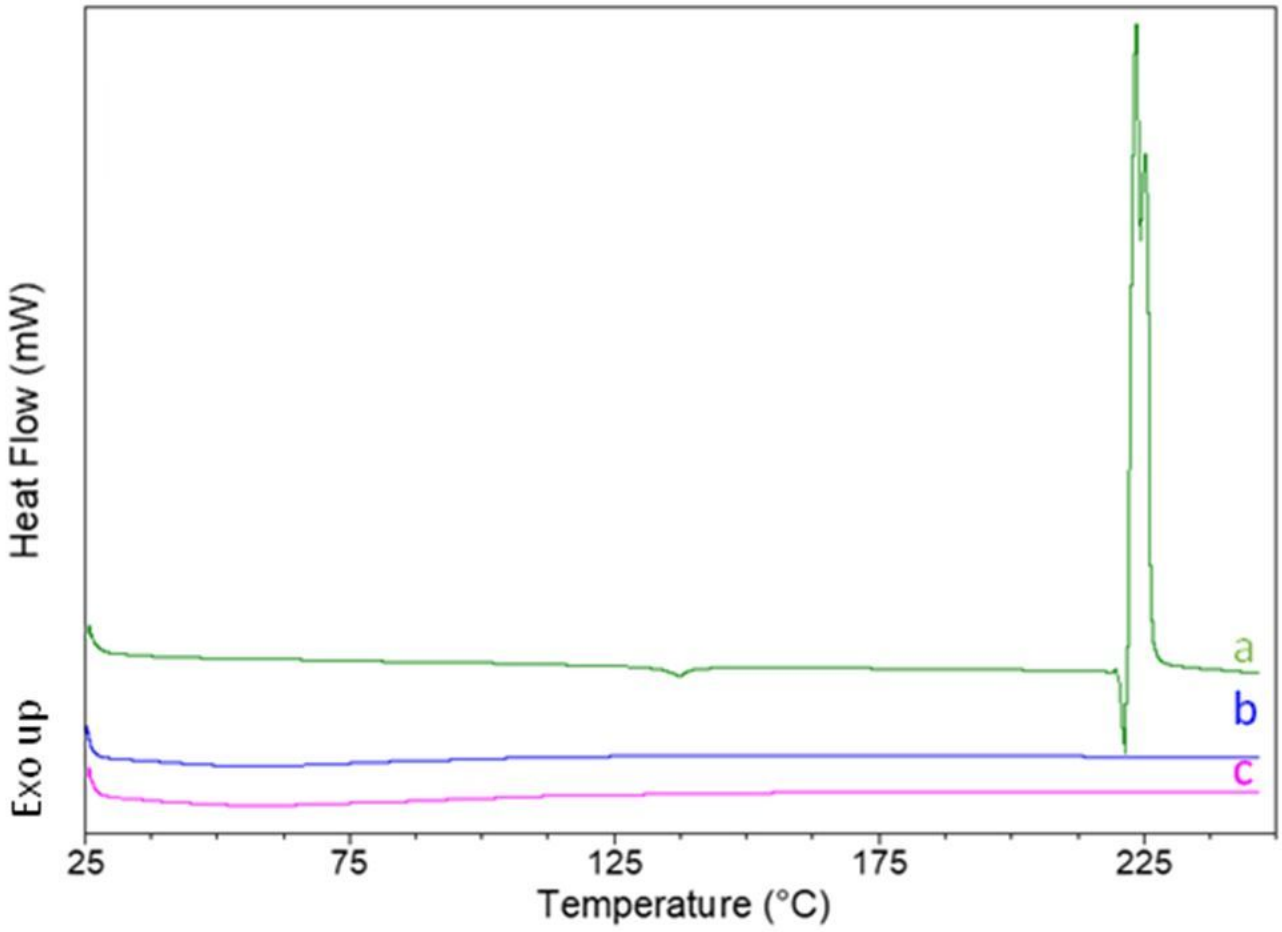

Figure 3

DSC curves of *Fur* (a), *HAP-Pure-Fur* (b) and *HAP-Sr-Fur* (c) samples.

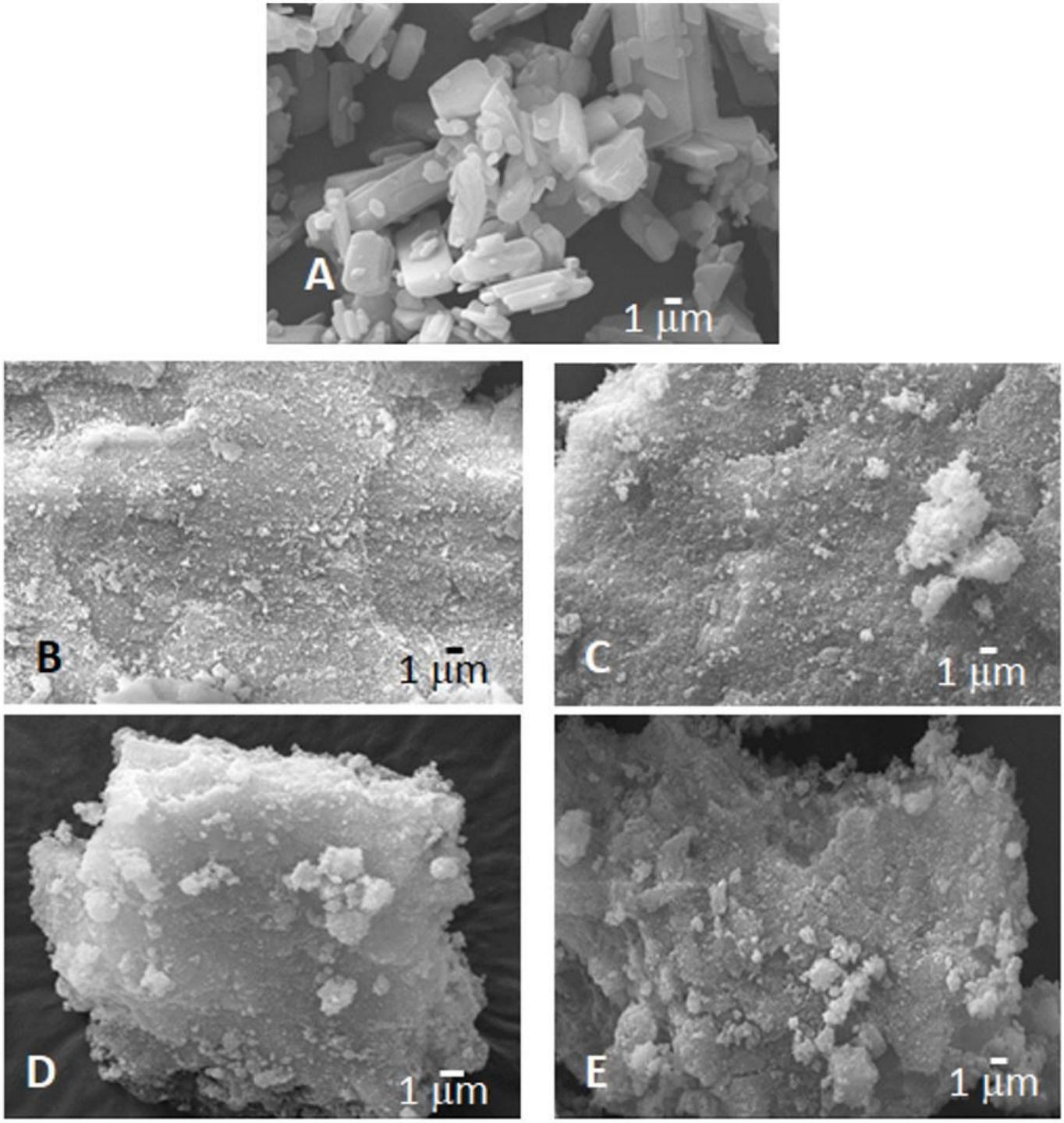

Figure 4

SEM micrographs, at 10 KX magnification, of (A) *Fur*, (B) *HAP-Pure*, (C) *HAP-Sr*, (D) *HAP-Pure-Fur* and (E) *HAP-Sr-Fur* samples.

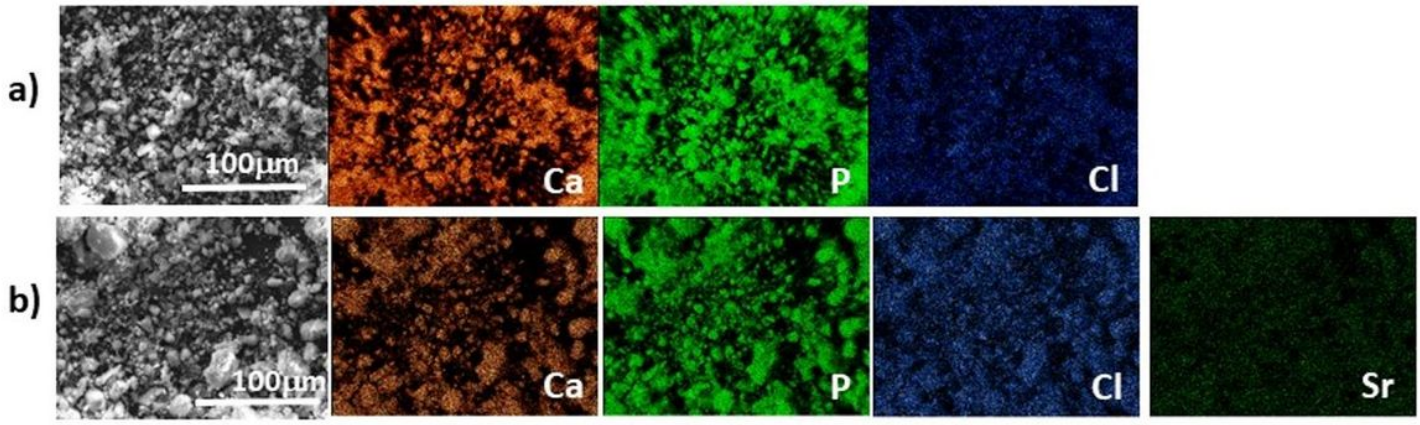

Figure 5

SEM micrographs and the corresponding elemental maps of the indicated elements for *HAP-Pure-Fur* (a) and *HAP-Sr-Fur* (b) samples.

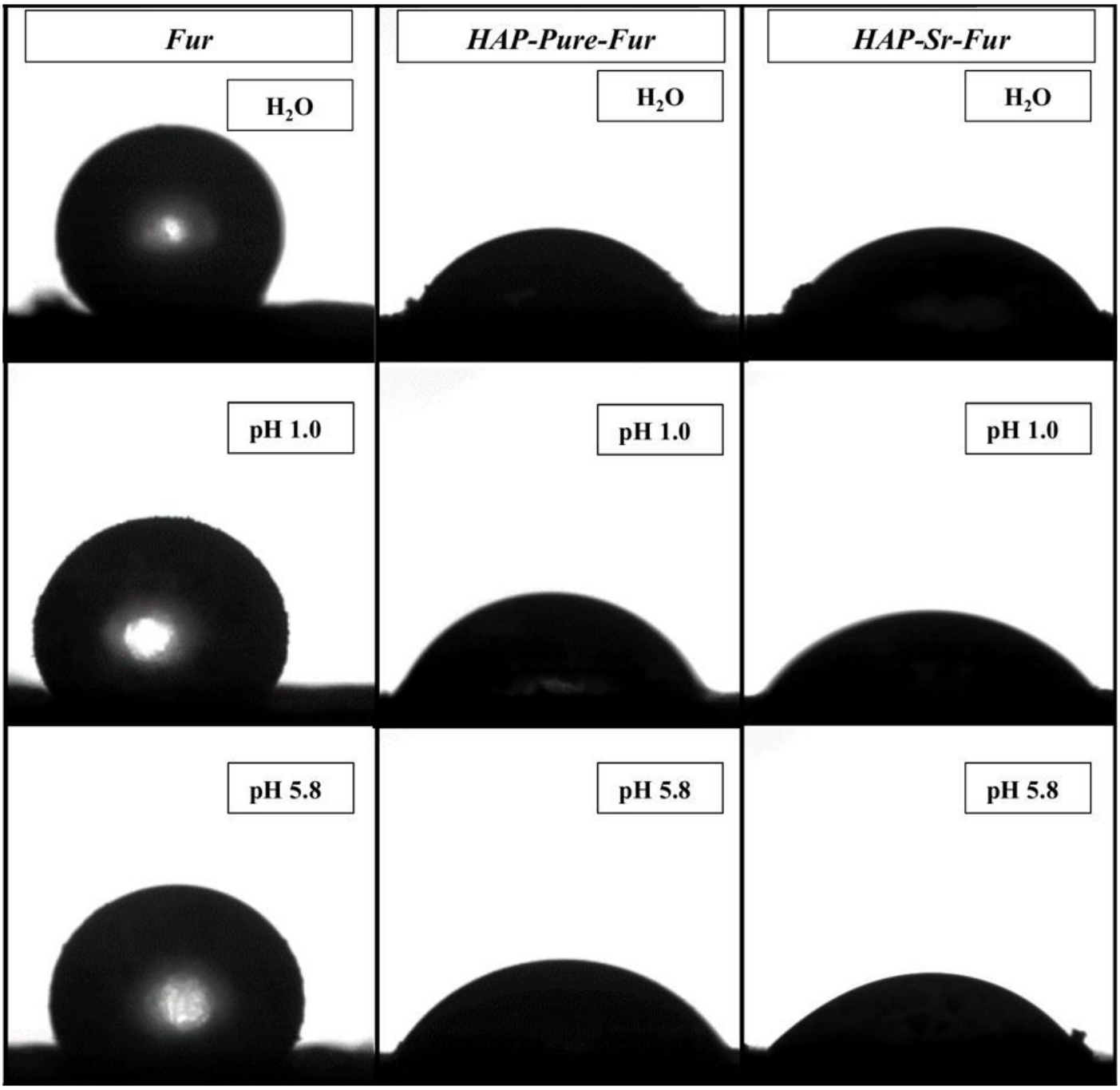

Figure 6

Images of the droplets used for the contact angle measurements: *Fur*, *HAP-Pure-Fur* and *HAP-Sr-Fur* in the different media, taken 1 sec after deposition.

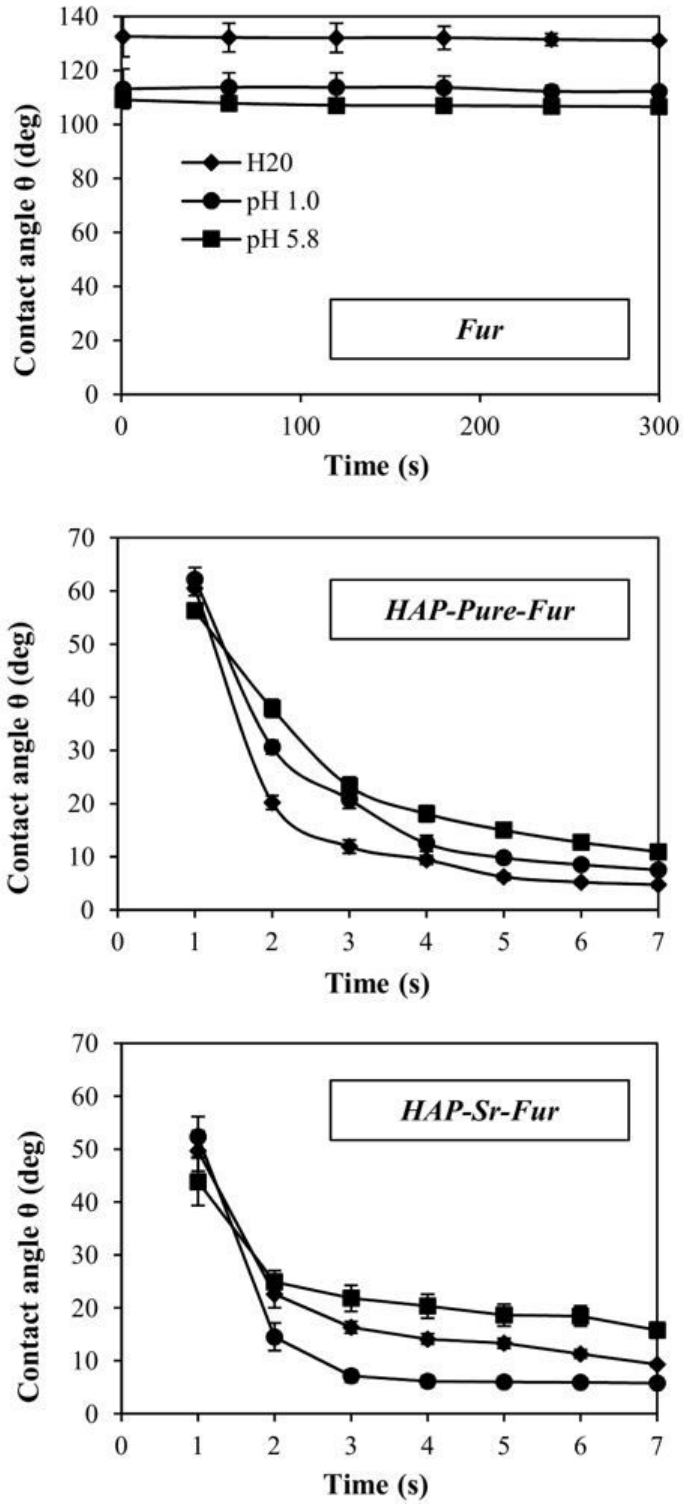

Figure 7

Contact angle values θ (deg) as a function of time for *Fur*, *HAP-Pure-Fur* and *HAP-Sr-Fur* in the different media considered.

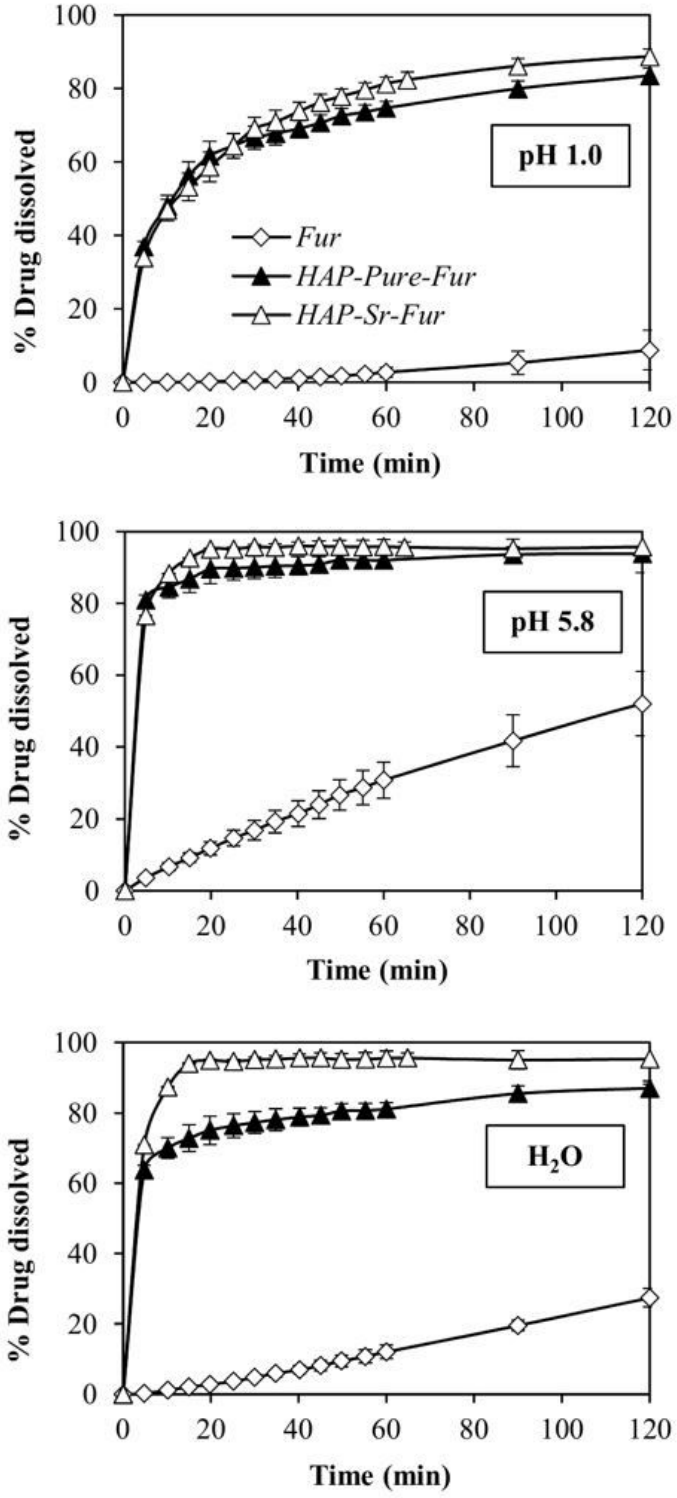

Figure 8

Dissolution profiles of free Furosemide (*Fur*), *HAP-Pure-Fur and HAP-Sr-Fur* in different media: pH 1.0, pH 5.8 (USP Monography) and deionized water (H_2O). All samples contain a dose of 25 mg of *Fur*.

Supplementary Files

This is a list of supplementary files associated with this preprint. Click to download.

- Scheme1.jpg